HYDRODYNAMICS AND HEAT TRANSFER IN COOLING SYSTEMS WITH INTERSECTING CHANNELS. II. HEAT TRANSFER AND TEMPERATURE FIELDS

Yu. I. Shanin, V. A. Afanas'ev, and O. I. Shanin

UDC 536.25:62-405.8

Results are provided of analysis and measurements of heat transfer and temperature fields at the numbers $Re_1 = 1 \cdot 10^2 - 2 \cdot 10^4$ and Pr = 5.5-8, depending on the geometry and angles of streamline structure.

Introduction

Heat transfer in cooling systems with intersecting channels has practicly not been investigated. There exist some data on the effective heat transfer of similar structures [1] under conditions of their one-sided thermal load, which are not generalized and are valid only in specific cases. For estimation calculations one uses dependences for heat transfer in short channels [2] or beam tubes [3], but their validity is not obvious and has not been verified experimentally.

In the present study we determine experimentally the temperature fields and heat transfer in cooling systems with intersecting channels, for which the hydroresistance was determined earlier [4].

Investigations of heat exchange were carried out on models of copper [No. 1-10, 13, 15, λ = 380 W/(m·K)] and molybdenum [No. 11, 12, 14, λ = 130 W/(m·K)] (the model number is the same as in [4]). Experiments were carried out based on the method of a thermal wedge, carried out on a copper prism with a heat exchange surface in the form of a rectangle of sizes 80 × 30 mm (with the 80-mm size along the model). The wedge was supplied with an Ohmic heater. Besides tightening, thermal contact between the wedge and the model was improved by distributing between them liquid-metal indium–gallium eutectic. Alternate heating was implemented experimentally both from the side of a monolithic plate, in which the channels are located, and from the side of the associated plate. The thermal flux was measured in four cross sections along the heater and the model with a temperature drop determined by means of 24 nickel–chromium thermocouples (see Fig. 1 of [4]). Eight thermocouples in isothermal directions are embedded in the model in the corresponding cross sections in the upper and lower plates. The temperature of the cooled surface of the model t_s was determined from the thermal flux and the model temperature by linear extrapolation. The distribution of heated water over the length of the heated portion of the model was taken to be linear for uniform specific thermal flux q_0, varying as a function of discharge within the range $q_0 = (1 - 4.5) \cdot 10^5$ W/m^2. Values of the reduced heat transfer coefficient α_{red} ($\alpha_{red} = q_0/(t_s - t_f)$, where t_f is the mean mass fluid temperature at the cross section of measurement) were determined experimentally for varying water discharge (Pr = 5.5-8), as well as of the "thermal isolation" coefficient of the lower plate K_{ti} ($K_{ti} = (t_0 - t_f)/(t_s - t_f)$, t_0 is the temperature of the lower thermally isolated plate). In the generalization we used a Reynolds number determined from the hydraulic channel diameter d_h and one of the velocities w_1 (Re_1), w_2 (Re_2) (for the detailed definitions of w_1, w_2, Re_1, Re_2 see [4]). The maximum errors in determining the various quantities did not exceed (3-5)% for q_0, (12-16)% for α_{red}, (5-6)% for Re, and (5-20)% for K_{ti}.

The quantities α_{red} and K_{ti} characterize the temperature field in the model. At the same time α_{red} is a characteristic of the effective heat transfer similarly to [1], and along with surface heat transfer of nonedged parts of the model (the mean heat transfer coefficient α_0) it includes the contribution to it of prismatic edges (the mean heat transfer coefficient α) and of the lower plate. In carrying out calculations of thermally deformed construction states

Translated from Inzhenerno-Fizicheskii Zhurnal, Vol. 61, No. 6, pp. 915-924, December, 1991. Original article submitted January 23, 1991.

provided by these cooling systems, one uses the coefficients α_{red} and K_{ti}, describing uniquely the temperature field. Besides, α_{red} characterizes integral heat exchange under conditions of a one-sided thermal load. The quantity K_{ti} is conditionally called the "thermal isolation" coefficient, indicates the ratio of excess temperatures of thermally isolated and thermally loaded plates, and characterizes the ratio of the thermal flux q_1, which would reach the foundation of the construction (in the absence of a thermal isolation boundary condition), to the total thermal flux q_0 (since $K_{ti} = (t_0 - t_f)/(t_s - t_f) = \alpha_{red}(t_0 - t_f)/[\alpha_{red}(t_s - t_f)] = q_1/q_0$). The α_{red}, K_{ti} values have been determined in the range of Reynolds numbers $50 \leqslant Re_1 \leqslant 2{,}5 \cdot 10^4$ and for various groups of models (Nos. 1-5, 6-10, 11-15, see Table 1 in [4]), in comparing which one can establish the effect of absolute sizes d_h (or the compactness K), the angle φ, and the heat conduction of the material λ. Inside the groups one usually investigates the action of the attack angle γ.

In the first group (models 1-5) there appear copper samples having sizes d_h = 2.0-2.4 mm, h_k = 2.0-3.0 mm and differing by the angle of attack (γ = 0-45°). The most informative change from the point of view of the functional behavior of $\alpha_{red} = f(Re)$ with increasing Re is observed for the corridor of the waffle system (models Nos. 1, 3, γ = 0°) (Fig. 1). As in the case of hydraulic resistance ξ, here there exist intervals of the Reynolds number (coinciding with the corresponding intervals as a function of $\xi(Re_1)$), in which the behavior of α_{red} differs qualitatively. The least intense α_{red} increases in the region of viscous flow ($Re_1 < 150$), and then the rate of growth is somewhat enhanced for viscous-inertial flow with predominance of viscosity. The largest growth rate in α_{red} is observed in the region of transition to turbulent flow, while in the turbulent region the growth rate in α_{red} is slowed down and becomes approximately stabilized (in which case the derivative $d\alpha_{red}/dRe_1$ tends to be slightly reduced in logarithmic coordinates). For rough walls (model No. 1) the portions of qualitative variation in α_{red} are weakly traced up to $Re_1 = 2 \cdot 10^3$, while for smooth walls (model No. 3) these regions are clearly expressed (Fig. 1). In the transition flow region ($1 \cdot 10^3 \leqslant Re_1 \leqslant 1{,}6 \cdot 10^3$) the increase in heat transfer in this system is proportional to complex $Re_1^{1.33}$. For increasing resistance by 1.5 times in this region the α_{red} value increases by more than twice at the end of the region than near its beginning, i.e., the increase in heat transfer leads the increase in resistance, and there exists a region of energetically favorable intensified heat transfer. Static pressure fluctuations of large amplitude, indicating flow instability and periodicity of its motion, were observed in this region of Re_1 numbers.

The heat transfer presented in the whole interval of Re_1 numbers ($1 \cdot 10^2 < Re_1 < 2 \cdot 10^4$) varied strongly ($4 \cdot 10^3 \leqslant \alpha_{red} \leqslant 1 \cdot 10^5$ W/m^2·K), though in the turbulent flow region $2 \cdot 10^3 \leqslant Re_1 \leqslant 2 \cdot 10^4$ this variation is not too substantial ($3 \cdot 10^4 \leqslant \alpha_{red} \leqslant 1 \cdot 10^5$ W/m^2·K). Compared with the initial system, for some typical sizes (d_h, h_k, δ_p = idem) [5] identical with the waffle system α_{red} for the waffle corridor system is 1.5 times higher ($Re_1 = 2 \cdot 10^4$), and this ratio is enhanced for decreasing Re_1. For models No. 1, 3 the variation in K_{ti} occurs smoothly in the whole Re_1 range from values close to 1 (for small Re_1) to $K_{ti} \approx 0.3$ (at $Re_1 = 2 \cdot 10^4$).

For increasing angle of attack γ (models No. 2, 4, 5) there is a qualitative change in the nature of heat transfer, and the rate of heat transfer ($d\alpha_{red}/dRe_2$) decreases for some increase in its absolute value (for identical Re_2 values). The maximum achieved is $\alpha_{red} \approx 1.2 \cdot 10^5$ W/(m^2·K) (for models No. 2, 5, with $Re_2 = 1 \cdot 10^4$). In the lower part of Re_2 numbers (corresponding to the viscous-inertial and viscous flow regimes, $Re_2 < 1.5 \cdot 10^3$) of the systems streamlined by the angle of attack (the limiting case of this flow is a checkered structure, γ = 45°) they have a (2-4)-fold advantage in α_{red} in comparison with the corridor structure (γ = 0°) (Fig. 1, model No. 5). With increasing γ the thermal isolation coefficient K_{ti} decreases and reaches values $K_{ti} = 0.14$ ($Re_1 = 10^4$), implying intensified surface heat transfer. To clarify the possibilities of local thermal modeling, model No. 2 was loaded with an axially symmetric thermal load with a patch diameter 25 mm. For $Re_2 > 3 \cdot 10^3$ the method provides results close to the case of a one-dimensional load, while for smaller Re_2 the results for α_{red} are enhanced, since the two-dimensionality of the temperature field starts being manifested in the thermally sensing plate of the model.

The application of a more finely ground structure of copper (models Nos. 6-10, $d_h \approx$ 1.65 mm, $h_k/\delta_p \approx$ 1.1-1.2) leads, for approximatley the same porosity, to an absolute increase in α_{red} for identical Re_2 compared to models 1-5 (Fig. 2). Independently of the angle of attack, for $\gamma > 15°$ and $Re_2 < 400$ and for models 6-10 α_{red} are approximately equal (it was earlier noted [4] that for $Re_2 \leq 200$ their resistance coefficients are practically identical).

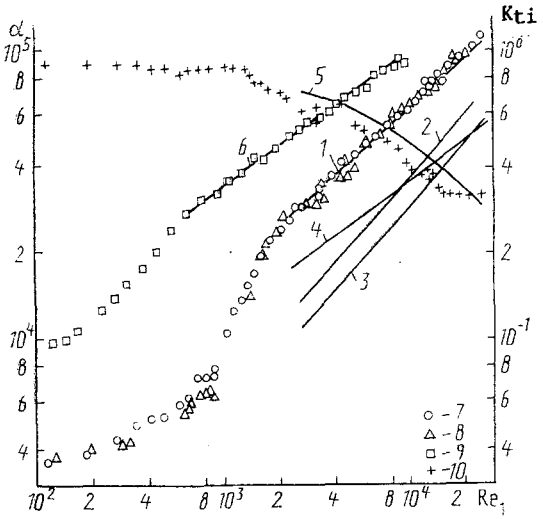

Fig. 1. The heat exchange characteristics of model No. 3 as a function of the Reynolds number: 1) $\alpha_{red} = 380.6\ Re_1^{0.59}$, W/(m²·K); 2) $\alpha_0 = 45.4\ Re_1^{0.727}$, W/(m²·K); 3) $\varepsilon\alpha_0$; 4) $\alpha_{red} - \varepsilon\alpha_0$); 5) Kti calc; 6) $\alpha_{red} = 1320\ Re_1^{0.47}$, W/(m²·K); 7-10) experiment: 7, 8) α_{red} (7, heated from the side of the associated plate; 8, from the side of the monolith), 9) α_{red} for model No. 5, 10) Kti exp.

The maximum is reached at $\alpha_{red} \simeq 1.4 \cdot 10^5$ W/(m²·K) for model No. 6 at $Re_2 = 1 \cdot 10^4$. For a total increase in compactness of this group of models by 1.5 times a relative increase was observed in heat transfer by 1.5-1.25 times for $0 \leqslant \gamma \leqslant 45°$, respectively. Consequently, the approximately proportional compactness of α_{red} is enhanced only for corridor waffle systems, while the dependence is weaker in the remaining cases.

The use of structures with a smaller angle of channel intersection φ ($\varphi = 60°$, models No. 13, 15) for the same material and in the checkered configuration ($\gamma = 30°$) in comparison with $\varphi = 90°$ leads to an absolute increase in α_{red} (by 10-15%). For these systems were also obtained substantial values of α_{red} ($\alpha_{red} = 1.2 \cdot 10^5$ W/(m²·K) for model No. 15 with $Re_2 = 5 \cdot 10^3$).

The use of a less thermally conducting construction material (models No. 11, 12, 14) reduces K_{ti} by several orders of magnitude ($K_{ti} = 0.02$-0.1), retaining in this case a high α_{red} ($\alpha_{red} = 1.15 \cdot 10^5$ W/(m²·K) for model No. 11 with $Re_2 = 7.5 \cdot 10^3$).

For such prototype systems was obtained a solution of the one-dimensional equation of heat conduction [5], which is correct for a homogeneous thermal flux, constant thermophysical properties of the material, and different heat transfer coefficients on edged α and nonedged surface α_0. The expressions for calculating the temperature field over the height of the model (plate–edge–plate) and α_{red} under condition $\text{th}\,\varphi = \varepsilon\alpha_0/[(1-\varepsilon)\lambda m] \leqslant 1$ are

$$\theta_I = \frac{\text{ch}\,\varphi}{1-\varepsilon}\,\frac{\text{ch}\,(mh_к + \varphi)}{\text{sh}\,(mh_к + 2\varphi)} + (h_1 - x)\,m, \tag{1}$$

$$\theta_{II} = \frac{\text{ch}\,\varphi}{1-\varepsilon}\,\frac{\text{ch}\,[m\,(h_2 - x) + \varphi]}{\text{sh}\,(mh_к + 2\varphi)}, \tag{2}$$

$$\theta_{III} = \frac{\text{ch}\,\varphi}{1-\varepsilon}\,\frac{\text{ch}\,\varphi}{\text{sh}\,(mh_к + 2\varphi)}, \tag{3}$$

$$\alpha_{red} = \varepsilon\alpha_0 + (1-\varepsilon)\,\lambda m\,\text{th}\,(mh_к + \varphi), \tag{4}$$

$$K_{ti} = \theta_{III}/\theta_I\,(x = h_1) = \text{ch}\varphi\,/\text{ch}\,(mh_к + \varphi), \tag{5}$$

where $\theta_i = \vartheta_i \lambda m/q_0$ is the dimensionless temperature (i = I, II, III), $\varepsilon = 1 - \delta_p^2/(\delta_k + \delta_p)^2$ is the porosity, $m = \sqrt{\alpha \Pi_p/(\lambda S_p)}$, Π_p and S_p are the perimeter and area of the transverse cross section of the edge, and $\text{th}\varphi = \varepsilon\alpha_0/[(1-\varepsilon)\lambda m]$. When $\varepsilon\alpha_0/[(1-\varepsilon)\lambda m] = \text{cth}\,\varphi > 1$ only the type of hyperbolic function changes its shape in (1)-(5): ch φ by sh φ, ch $(mh_к + \varphi)$ by sh $(mh_к + \varphi)$ and th φ cth φ.

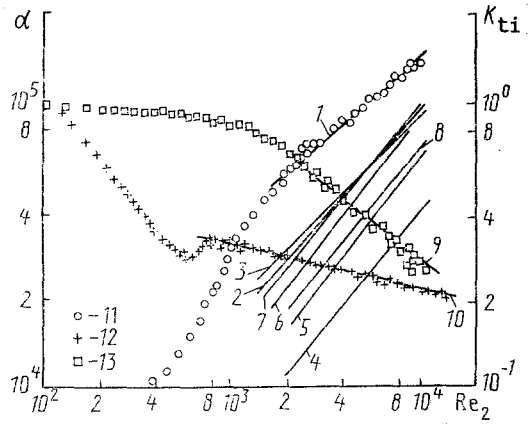

Fig. 2. Thermal characteristics in model No. 6 in relation to Reynold's number: 1 – $\alpha_{red}=721\ Re_2^{0,573}$, Вт/(м²·К); 2 – $\alpha_0 \simeq 107\ Re_2^{0,73}$, Вт/(м²·К); 3- function α_0 for cluster pipe tube with identical dimensions d_h, $\bar{S}_2$, $\bar{S}_1$ [3]; 4 – $\alpha_0=26\ Re_2^{0,8}$ ($Nu=0{,}021\ Re_1^{0,8}Pr^{0,43}$ formula 7; 5 – function for heat emission in a brief channel [2]; 6, 7) function for a brief channel in T = 20 and 30% [2]; 8 – formula $Nu=0{,}055\ Re^{0,78}Pr^{0,33}$ [8]; 9 – Calculation value K_{th} in $\alpha \approx \alpha_0$; 10 – $\xi=0{,}72\ Re_2^{-0,12}$; 11-13 – experiment: 11 – α_{red}, Вт/(м²·К); 12 – ξ_2; 13 – K_{ti} calc.

The effect of geometric parameters and material construction on heat exchange by using (1)-(5) cannot be analyzed until α_0, α are known. Flow visualization (and the heat transfer related to it) in the corridor waffle system ($\varphi=90°$) shows that the distribution of α over the edge perimeter is nonuniform. In the turbulent flow regime the most intense heat transfer ($\sim Re^{0.8}$) can be anticipated at the edge from the side of the circulating channel. In analogy with tubular corridor beams, for which the zone of separated and stagnant flow is large, the heat transfer coefficient at the boundaries, converting to stagnant zones, must depend to some extent on the flow velocity ($\sim Re^{0.6}$). Therefore, for highly thermally conducting edges ($Bi = \alpha S_p/\Pi_p\lambda < 0.1$) for the mean over the perimeter α one can expect a dependence of heat transfer on the flow velocity $\sim Re^{0.7-0.75}$. The heat transfer of a checkered structure, having diagonal symmetry of streamlines, being most intense at the leading boundary, must be reduced at the separation zone at the second boundary, and in analogy with the checkered beam tube can be expected to follow the relation $\alpha \sim Re^{0.6-0.65}$. A similar dependence on the velocity w can be expected for α_0. For finite-size structures the experimental investigation of local heat transfer is difficult to implement, therefore in the following we assume constancy of the averaged α, α_0 (determined empirically) over the areas. It has been shown in [6] that for a rectangular channel the heat transfer coefficient α_s, averaged over the perimeter and found as a result of solving the associated problem of heat exchange, despite the complicated nature of the distribution of the local heat transfer coefficient in the turbulent flow region of heat carriers is in good agreement with Mikheev's empirical equation [7], describing heat transfer in prismatic channels.

Based on the experimental data of $\alpha_{red}(Re)$, $K_{ti}(Re)$, from (1)-(5) one can uniquely identify α, α_0, α_v:

$$\frac{mh_к}{\mathrm{sh}\,(mh_к)} = \frac{\alpha_{red}}{\lambda(1-\varepsilon)\left(\dfrac{\vartheta_s}{\vartheta_0}\dfrac{\vartheta_0}{\vartheta_s}\right)}, \tag{6}$$

$$\alpha_0 = \frac{1-\varepsilon}{\varepsilon}\lambda m \frac{\dfrac{\vartheta_s}{\vartheta_0} - \mathrm{ch}\,(mh_к)}{\mathrm{sh}\,(mh_к)}, \tag{7}$$

$$\alpha_v = \lambda m^2 (1-\varepsilon). \tag{8}$$

The practice of using expression (6) to determine the complex $mh_к$ has shown a strong dependence on the error of determining α_{red}, K_{ti}. The absence of smoothing of experimental results and systematic measurement errors have led to "buildup" in α, α_0 and to possible loss

of physical meaning of the values obtained (negative α_0), caused by the behavior of the function $mh_k/sh(mh_k)$. The introduction of piecewise approximations of α_{red} by power-law functions $\alpha_{red} = A_1 Re_2^{n_1}$ and the determination of A_1, n_1 by the least squares method have made it possible to reduce the "buildup," but credible data are obtained only in the case of highly accurate determination of α_{red}, K_{ti}. With account of our errors in determining α_{red}, K_{ti} of acceptable results it was possible to add to the approximation $\alpha \approx \alpha_0$ for all models, so that for relatively small edge sizes and complicated three-dimensional flows the flow is physically correct. The relation $\alpha_0 \simeq \alpha = A_2 Re_2^{n_2}$ has been obtained as a result of solving Eq. (4). The verification of reliability of the assumption $\alpha \approx \alpha_0$ was provided by the correspondence between $K_{ti\ calc}$ and $K_{ti\ exp}$ (including the error in determining $K_{ti\ exp}$) for all models, and the direct experiment was carried out on model No. 16. A corridor waffle system was recently formed in a plastic plate in which, following the visualization of [4], a thermal load of a copper plate was attached to the plastic cover. Its heat transfer (α_0) was determined for $170 < Re_1 1.2 \cdot 10^4$, while in the turbulent flow region ($2 \cdot 10^3 < Re_1 \leqslant 1{,}2 \cdot 10^4$) the results are generalized by the dependence

$$Nu_0 = \frac{\alpha_0 d_h}{\lambda_f} = 0{,}175\, Re_1^{0{,}727}, \tag{9}$$

practically coinciding on the plot $\alpha_0(Re)$ with the dependence obtained from (4) for the single-type model No. 3:

$$Nu_0 = 0{,}13\, Re^{0{,}748}. \tag{10}$$

The heat transfer data are generalized as $K_1 = NuPr^{-1/3} = A_3 Re_1^{n_2}$, and are represented in Table 1 in the operating interval (A_2, n_2 are shown without dispersion deviations). The surface heat transfer coefficients are characterized by high values at the maximum achieved Re numbers ($\alpha = (6\text{-}9) \cdot 10^4$ W/(m²·K) for $Re_1 = (1\text{-}2) \cdot 10^4$). At $\varphi = 90°$ and for the model groups No. 1-5, 6-10 the exponents are $n_2 \simeq 0{,}73$ ($\gamma = 0°$) and $n_2 \simeq 0{,}6$ ($\gamma = 45°$). The absolute value of α increases with γ for constant Re and for a fragmented structure. Maximum heat transfer is noted for checkered structures (models No. 10, 14) and for structures washed under high angles of attack (γ = 40, 30°), which are closest to checkered structures. Compared to the corridor, the checkered structure enhances heat transfer by several times at low Re, which is explained by the earlier manifestation of the inertial flow regime in them. A decrease in φ leads to a change in streamlines and, as a consequence, to an increase in n_2 for the checkered structures Nos. 12-15 up to 0.62-0.65; they have a less strongly expressed dependence of heat transfer on the angle of attack. For models No. 11, 14 with rough walls one obtains a maximum $\alpha \simeq 9 \cdot 10^4$ W/(m²·K). For decreasing porosity ε a tendency is noted toward reduced α.

Comparison of the heat transfer of waffle corridor structures with the heat transfer of channel cooling systems ($K_1 \simeq 0.021\, Re_1^{0{,}8}$) in K_1–Re_1 coordinates has revealed substantial differences in the turbulent flow region (Fig. 2). Applying the equations of heat transfer in short channels [2, p. 188] to model No. 6 shows an increase in heat transfer by 1.6 times, but it is poorly approximated (Fig. 2). Taking into account the turbulence of the advancing flow, the heat transfer in short channels is even more intensified [2, p. 193]. The variation in the extent of flow turbulence T in the range 10 < T < 30% leads to an increase in heat transfer by 1.1-1.5 times, and for large turbulization (T ≃ 30%) a correlation is observed with heat transfer of tubular corridor beams [3, p. 130].

If the base of the variant is selected to be a corridor waffle structure (models No. 1, 3, 12, 6], it is seen that with some tension (usually toward the side of enhancement) for its heat transfer one can use the dependence for tubular corridor beams [3] or for short channels [2] with T ≃ 20-30% (providing some reduction).

For heat transfer with a nonedged surface of a brush cooling system (cylindrical edges of relative length $h_к/d \simeq 7\text{--}9$, contained between two plates), being in a certain sense the analog of a waffle structure, an equation was obtained in [8], which correlates well with heat transfer in short channels with T = 10% [2].

For $\varphi = 90°$ an increase in the angle of attack γ (γ = 0-45°) leads to an increase in heat transfer by 1.5-1.7 times for a resistance increase by 10-15 times. The measurement of heat transfer in cases of axial symmetry of streamline structures only enables its determination for an arbitrary angle ($0 \leqslant \gamma \leqslant 45°$, $\bar{\gamma} = \gamma/45$):

TABLE 1. Generalization of Experimental Results on Hydroresistance and Heat Transfer in the Turbulent Region of Re Numbers

Model number	Resistance		Heat transfer α_{red}		$\alpha(Re_2)$	$K_1(Re_1)$	$K_D(Re_1)$	$K_\xi(\xi Re^3)$
	Range of Re	A_0; n_0	Range of Re	A_1; n_1	A_2; n_2	A_3; n_3	A	A_4; n_4
1	$(1,2—12)\cdot10^3$	0,4; 0	$(1,2—12)\cdot10^3$	911; 0,5	156; 0,636	0,23	114,5	0,38; 0,212
2	$(2—10)\cdot10^2$	8,3; 0	$(2—10)\cdot10^2$	4592; 0,38	1003; 0,508	1,66	829,0	1,415; 0,17
3	$(2—20)\cdot10^3$	0,635; —0,093	$(2,5—25)\cdot10^2$	380,6; 0,59	67; 0,727	0,09	40,8	0,13; 0,25
4	$(6—100)\cdot10^2$	1,3; 0	$(3,5—100)\cdot10^3$	1354; 0,48	230; 0,625	0,37	195,0	0,45; 0,21
5	$(4—80)\cdot10^2$	2,47; 0	$(4—70)\cdot10^2$	1621; 0,47	245; 0,627	0,39	202,7	0,42; 0,21
6	$(8—150)\cdot10^2$	0,72; —0,12	$(2—16)\cdot10^3$	721; 0,573	107; 0,733	0,115	71,6	0,165; 0,255
7	$(3—60)\cdot10^2$	1,9; 0	$(3—40)\cdot10^2$	1004; 0,556	178; 0,7	0,196	123,5	0,22; 0,233
8	$(2—40)\cdot10^2$	4,74; —0,06	$(3—40)\cdot10^2$	1285; 0,543	243; 0,68	0,27	171,0	0,244; 0,231
9	$(4—60)\cdot10^2$	3,6; 0	$(4,5—30)\cdot10^2$	973; 0,586	180; 0,73	0,165	105,5	0,233; 0,232
10	$(4—40)\cdot10^2$	4; —0,002	$(4—30)\cdot10^2$	2586; 0,464	537; 0,6	0,63	384,0	0,596; 0,2
11	$(1—10)\cdot10^3$	2,12; —0,164	$(1—10)\cdot10^3$	1700; 0,475	258; 0,65	0,28	252,0	0,314; 0,23
12	$(1—10)\cdot10^3$	0,41; 0	$(1—8)\cdot10^3$	1387; 0,46	181; 0,644	0,2	175,5	0,313; 0,215
13	$(5—60)\cdot10^2$	1,7; —0,08	$(5—45)\cdot10^2$	2834; 0,434	241; 0,632	0,23	217,7	0,28; 0,217
14	$(1,4—40)\cdot10^2$	3,14; —0,12	$(6—60)\cdot10^2$	1762; 0,48	335; 0,646	0,41	330,0	0,41; 0,224
15	$(1—14)\cdot10^3$	1,2; —0,022	$(1,6—14)\cdot10^3$	2704; 0,44	314; 0,616	0,234	257,7	0,44; 0,207
16	—	—	$(2—12)\cdot10^3$	54,6; 0,71	—	0,094	47,1	—

$$\mathrm{Nu}_\gamma = C_0 C(\bar{\gamma})\left[1+\left(\frac{\mathrm{Nu}_{45}}{\mathrm{Nu}_0}-1\right)\bar{\gamma}\right]\mathrm{Pr}^{1/3}\,\mathrm{Re}_1^{n_0+\bar{\gamma}(n_{45}-n_0)} \tag{11}$$

and allows to specify its applicability to the group of models No. 6-10 (Fig. 3)

$$K_1 = \mathrm{Nu}_\gamma \mathrm{Pr}^{-1/3} = 0{,}115(1+2\bar{\gamma})(1+0{,}7\bar{\gamma})\,\mathrm{Re}_1^{0{,}73-0{,}13\bar{\gamma}}. \tag{12}$$

At $\varphi=60°$ an increase in γ (γ = 15-30°) leads to an increase in resistance by 1.3-2 times for an approximately constant increase of heat transfer of Nu_γ by 1.4-1.5 times. The heat transfer of checkered structures correlates with the heat transfer in spherical fillings [9], implying definite analogy of hydrodynamic processes in these structures.

For the bulk heat transfer coefficient α_v ($\alpha_v=\alpha\Pi_p(1-\varepsilon)/S_p$) the results (in coordinates K_V–Re_1, $K_V = \mathrm{Nu}_V\mathrm{Pr}^{-1/3} = A\mathrm{Re}_1^n$, $\mathrm{Nu}_V = \alpha_V d_h/\lambda_f$ of Table 1) are even more distinct for corridor and checkered structures, among which the top places are occupied by structures with smaller φ (models No. 11, 14). To implement these K_V values in channel, as well as waffle, systems they must have channel and edge sizes smaller by 3-6 times (at identical height).

Based on the knowledge of α resulting from analyzing α_{red}, we note two facts: firstly, for waffle structures with porosity ε = 0.75 the component distributions to α_{red} are redistributed in comparison with channel structures (ε = 0.5), i.e., the contribution of a non-edged surface $\varepsilon\alpha_0$ increases, while that of an edged surface drops, so that their relative weights become approximately equal; secondly, due to the large surface heat transfer (in comparison with a channel system) for waffle systems identical with a channel system α_{red} [5] can be 2-3 times larger for characteristic sizes of d_h, δ_k, being at the same time a source of growth of α_{red} for finely divided structures.

To explain the energetic effectiveness of the systems investigated and search for the mutual relationship between the hydraulic resistance and heat transfer in structures with complicated topology on the basis of the method of local similarity and the Kolmogorov velocity scale in analogy with [10], the results in the indicated Re range are represented in the form of power functions $K_\xi(\xi\mathrm{Re}^3)$ [$K_\xi=\mathrm{NuPr}^{-1/3}=A_4(\xi\mathrm{Re}_3^2)^{n_4}$] (Table 1). In the coordinates K_ξ – $\xi_2\mathrm{Re}_2^3$ the results consist of a band with approximtely identical ratio of maximum (model No. 14) to minimum K_ξ (model No. 13) equal to ~1.85 in the whole range of variation of $\xi_2\mathrm{Re}_2^3$ ($10^9\leqslant\xi_2\mathrm{Re}_2^3\leqslant10^{12}$). The exponent n_4 varies in the range 0.2-0.255 (the larger exponents correspond to the corridor structure, and the smaller – to checkered structures), with the constant being $0{,}13\leqslant A_4\leqslant0{,}6$. Comparison of the integral energetic effectiveness $\alpha_{red} = f(\Delta p/\ell)$ for the systems considered has shown that it is highest for model No. 6 (corridor structure), and then follow models No. 11, 14, 15 ($\varphi=60°$, $\gamma=30°$). For the remaining models the effectiveness consists approximately of a band where the ratio of the highest to lowest values does not exceed 1.2. For checkered structures the effectiveness with respect to the corridor is enhanced for decreasing pressure gradient The effectiveness of surface heat exchange [$\alpha(\Delta p/\ell)$] is most sharply manifested for checkered structures (models No. 14, 11, 10) in the whole range of $\Delta p/\ell$ (particularly strongly for low $\Delta p/\ell$). For $\Delta p/\ell \geq 10^6$ Pa/m, gain in the surface heat transfer for increasing γ is approximately compensated by a loss in hydroresistance (models No. 1-5, 6-10).

The intensifying effect on the reduced heat transfer of an edge with varying porosity can be analyzed by Eq. (4), dividing it by α_0 and selecting ε as the argument:

$$K_{in} = \frac{\alpha_{red}}{\alpha_0} = \frac{1-\varepsilon}{D_0}\,\frac{(1-\varepsilon)\,\mathrm{th}\,D_0\bar{h}+\varepsilon D_0}{(1-\varepsilon)+\varepsilon D_0\,\mathrm{th}\,\bar{h}}+\varepsilon, \tag{13}$$

where $D_0 = [\mathrm{Bi}_0 f(\varepsilon,\bar{h})]^{0,5}$, $f(\varepsilon,\bar{h}) = [\sqrt{1-\varepsilon}\,(\bar{h}-4)+4]\,[8\bar{h}(1-\sqrt{1-\varepsilon})]^{-1}$, $\mathrm{Bi}_0 = A_1\mathrm{Re}^{n_1}\mathrm{Pr}^m/\Lambda$, $\Lambda = \lambda/\lambda_f$, $\bar{h} = h_k\Pi_p/S_p$.

The curve $K_{in}(\varepsilon, \mathrm{Re})$ has an optimum, depending on the construction material, the flow regime, and the operating portion of Re numbers ($\mathrm{Re}\approx(0.5\text{-}1)\cdot10^4$), and is mildly sloping with a maximum in the interval $0.5 < \varepsilon < 0.8$ (Fig. 4). With decreasing heat conduction coefficient λ K_{in} decreases, similarly to the behavior for increasing Re numbers. An edge of different copper models with $\mathrm{Re}\simeq10^4$ provides approximately the same relative contribution to α_{red}. For specific porosity in the turbulent region of Re numbers K_{in} is determined by the function $K_{in} = (A_1/A_2)\mathrm{Re}_2^{(n_1-n_2)}$, and is represented by a straight line in semilogarithmic coordinates.

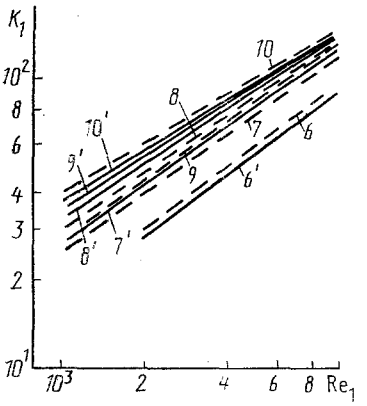

Fig. 3

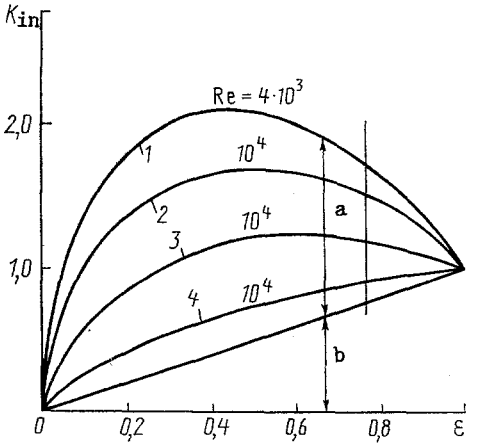

Fig. 4

Fig. 3. The surface heat transfer for models No. 6-10 (with numbers corresponding to curves) as a functon of the Reynolds number: 6-10) empirical equations, 6'-10') according to Eq. (12).

Fig. 4. The intensification coefficient K_{in} as a function of porosity ε (13) for sizes corresponding to model No. 6: 1, 2) λ = 380 W/(m·K); 3) 130; 4) 15; a) contribution to reduced heat transfer of edge portion of the system; b) contribution of nonedged portion of upper plate; the vertical line corresponds to ε = 0.77.

Based on the results of alternate determination of the reduced heat transfer coefficient from the monolithic side α_{red} and the associated plate $\alpha_{red}(R_T)$ (see Fig. 1), one can estimate the technological performance of a component, defining the thermal contact resistance R_T from the equation:

$$R_T = \alpha_{red}(1 - K_a)/[(K_a\alpha_{red} - \varepsilon\alpha_0)\lambda m], \tag{14}$$

where $K_a = \alpha_{red}(R_t)/\alpha_{red}$.

The experimentally established deviation for the models of 5-10% between α_{red} and $\alpha_{red}(R_T)$ is related only to the solder thermal resistance ($R_T \simeq (0.5\text{-}1.0)\cdot 10^{-6}$ m²·K/W), and corresponds to the good quality of the compound for waffle structures. The increase in contact resistance (due to oxide films, poorly prepared surfaces) does not lead for these structures to substantial reduction in the effectiveness of edges, which is so characteristic of channel systems.

Conclusion. Further enforcement of the thermohydraulic characteristics (α_{red}, α, ξ) of waffle cooling systems can be realized in a finely divided structure by retaining a large transverse thermally conducting skeleton, increasing the compactness, optimizing the porosity, decreasing the angle φ for a checkered edge, and using multistage systems with nonhighly thermally conducting edges.

NOTATION

d_h, hydraulic diameter of the channel, $d_h = 4F_k\Pi_k$; F_k, Π_k, transient area and parameter of the channel; δ_k, width of the channel; φ, γ, angles of channel intersection and of attack; ε, porosity, i.e., the ratio of volumes of vacancies to the total volume of the elementary unit cell of the cooling system; w_f, filtration rate; $w_1 = w_f/\varepsilon_m$, $\varepsilon_m = \delta_k/(\delta_p + \delta_k)$, $w_2 = w_f/\varepsilon$; $K = 4/\delta_p - 2\varepsilon(2/\delta_p - 1/h_k)$, compactness, i.e., the ratio of surface heat exchange to the volume of the elementary unit cell of the cooling system; ξ, hydraulic resistance coefficient; $\Delta p/\ell$, pressure gradient; α_{red}, α, α_0, α_v, the heat transfer coefficients (reduced, on the edge, on the nonedged part of the plate, bulk); q_0, specific thermal flux; t, temperature; $\vartheta = (t - t_f)$, excess temperature; λ_h, λ_f, heat conduction coefficients of the material and of the fluid; $Re_i = d_h w_i/\nu_f$, Reynolds number; and Pr, the Prandtl number.

LITERATURE CITED

1. V. V. Kharitonov, Thermophysical Calculations of Laser Mirrors [in Russian], Moscow (1985).
2. A. S. Sukomel, V. I. Velichko, and Yu. G Abrosimov, Heat Exchange and Friction in Turbulent Gas Flow in Short Channels [in Russian], Msocow (1979).
3. A. Zhukauskas, V. Makaryavichyus, and A. Shlanchyauskas, Heat Transfer of Tubular Beams in Transverse Fluid Flow [in Russian], Vil'nyus (1968).
4. Yu. I. Shanin, V. A. Afanas'ev, and O. I. Shanin, Inzh.-fiz. Zh., 61, No. 5, 717-725 (1991).
5. V. N. Fedoseev, O. I. Shanin, Yu. I. Shanin, and V. A. Afanas'ev, Teplofiz. Vys. Temp., 27, No. 6, 1132-1138 (1989).
6. Caddle and Sparrow, Teploperedacha, No. 1, 15-24 (1986).
7. M. A. Mikheev and I. M. Mikheeva, Fundamentals of Heat Transfer [in Russian], Moscow (1973).
8. V. I. Subbotin, V. V. Kharitonov, A. A. Plakseev, and S. V. Alekseev, Teploenergetika, No. 1, 42-44 (1985).
9. R. G. Bogoyavlenskii, Hydrodynamics and Heat Exchange in High-Temperature Nuclear Reactors with Spherical Fuel Elements [in Russian], Moscow (1978).
10. V. N. Fedoseev, V. I. Subbotin, and V. V Kharitonov, Teploenergetika, No. 6, 61-64 (1987).

UNROLLING OF MACROMOLECULES UNDER THE CONDITIONS OF WALL TURBULENCE

V. G. Pogrebnyak, Yu. F. Ivanyuta, and N. V. Naumchuk

UDC 532.517.4:539.199

The results of polarization–optical studies of turbulent wall flow of a solution of polyethylene oxide are presented, showing the existence of strong deforming action of the hydrodynamic field on macromolecules in certain zones of the boundary layer.

It has been shown experimentally [1-3] that macromolecules are subject to strong (up to 100%) unrolling in laminar streams with stretching. Macromolecules that are unrolled under the action of the longitudinal hydrodynamic field affect the structure of that field and cause a considerable increase in energy dissipation [4]. The influence of the unrolling macromolecules on the structure of the hydrodynamic field that unrolls them occurs at the molecular level in dilute polymer solutions and at the supermolecular level in semidilute and moderately concentrated solutions [3]. These results are decisive for the interpretation of the Toms effect. The lack of adequate experimental confirmation of the significant unrolling of macromolecules under the conditions of wall turbulence lowers their value, however.

Experimental data [5, 6] indicate that in a turbulent stream near a wall there are zones containing both elements of shear flow and flow elements (jet ejections) with stretching, which have their own time dynamics. The turbulence associated with ejections is considered to be primary, while the turbulence due to the instability and breakup of jets (liquid ejections) is secondary. The latter is very important, since in this case it is sufficient to reduce the frequency of ejections to ultimately reduce the frictional resistance.

It can be assumed that flow in the immediate vicinity of a wall, as in the case of laminar shear flow, should hardly change; at the same time, with increasing distance from the wall, where jet flows with large longitudinal velocity gradients start to occur, unrolling of macromolecules with all its consequences should be observed. Experiments showing the unrolling of macromolecules under the conditions of wall turbulence are therefore fundamental,

Donetsk Institute of Soviet Commerce. Translated from Inzhenerno-Fizicheskii Zhurnal, Vol. 61, No. 6, pp. 925-927, December, 1991. Original article submitted March 14, 1991.

0022-0841/91/6106-1475 $12.50